Directly Linked Porphyrin Arrays with Tunable Excitonic Interactions

ARTICLE *in* ACCOUNTS OF CHEMICAL RESEARCH · NOVEMBER 2004

Impact Factor: 22.32 · DOI: 10.1021/ar030242e · Source: PubMed

2 AUTHORS:

Dongho Kim
Yonsei University
500 PUBLICATIONS **13,564** CITATIONS
SEE PROFILE

Atsuhiro Osuka
Kyoto University
656 PUBLICATIONS **16,673** CITATIONS
SEE PROFILE

VOLUME 37 NUMBER 10

ACCOUNTS of CHEMICAL RESEARCH®

OCTOBER 2004

ARTICLES

Directly Linked Porphyrin Arrays with Tunable Excitonic Interactions

DONGHO KIM*,† AND ATSUHIRO OSUKA*,‡

National Creative Research Initiatives Center for Ultrafast Optical Characteristics Control and Department of Chemistry, Yonsei University, Seoul 120-749, Korea, and Department of Chemistry and Core Research for Evolutional Science and Technology (CREST), Kyoto University, Kyoto 606-8502, Japan

Received February 26, 2004 (Revised Manuscript Received June 8, 2004)

ABSTRACT

On the basis of the Ag(I)-promoted coupling reaction of Zn(II) 5,-15-diaryl porphyrin that gave a meso−meso-linked diporphyrin, we developed a variety of directly linked porphyrin arrays including linear, windmill, gridlike, cyclic, and box architectures. Electronic and excitonic interactions are thus fine tuned by placing porphyrin chromophores in well-defined arrangements. Photoexcited-state dynamics of these porphyrin arrays, as revealed by various ultrafast laser-based measurements, are pertinent to photosynthetic light-harvesting antenna in terms of very efficient excitation energy hopping over many porphyrins and lack of a defect that acts as energy sink. The conformational flexibility of a meso−meso-linked diporphyrin has also been used for the fine tuning of excitonic interactions as demonstrated by strapped meso−meso diporphyrins and reversible switching of energy transfer in a triporphyrin. Triply linked porphyrin arrays have also been explored, which exhibit an exceptionally low HOMO−LUMO gap as a result of a fully conjugated π electronic system over a coplanar platform.

1. Introduction

Photosynthesis is initiated by absorption of light, which is followed by excitation energy transfer (EET) to the reaction center. These sequential events occur in the light-harvesting antenna complexes that consist of regularly arranged photosynthetic pigments as seen in LH1 and LH2.[1,2] Considerable efforts have been made for exploration of multiporphyrin arrays with a view of not only duplicating the photosynthetic light harvesting antenna complexes but also possible applications such as molecular conductive wires and optoelectronic devices.[3]

Multiporphyrin arrays have been envisaged and prepared using several types of shorter linkers that are suitable for preparing linear or extended architectures via a meso position attachment (Chart 1).[4] During the past decade, various synthetic strategies have been developed in order to make multiporphyrin oligomers with linear, cyclic, and cross-linked geometries, which include porphyrins joined by ethene, ethyne, butadiyne, furan, enyne, hexatriene, *p*-phenylene, phenylethene, naphthalene, biphenyl, phenanthrene, and ethynylphenylethyne groups. Although there exist opulent molecular architectures due to various linkers to adjoin the porphyrin moieties together, the requirements for ample electronic interactions between neighboring porphyrin pigments for efficient energy transfer and well defined and rigid molecular structures to be void of any energy or charge sink should be considered. In this context, the porphyrin arrays where constituent porphyrins are connected directly without any links can be promising molecular architectures for the application of molecular photonic and electronic wires.

This Account deals with the synthesis and excited-state photophysics of directly linked porphyrin arrays that have

* To whom correspondence should be addressed.
† Yonsei University.
‡ Kyoto University.

Dongho Kim (b. 1957) grew up in Seoul, Korea. He received a B. S. in chemistry from Seoul National University in 1980 and a Ph. D. from Washington University in 1984. After postdoctoral research at Princeton University, he joined the Korea Research Institute of Standards and Science 1986. He moved to Yonsei University in 2000, where he is Professor of Chemistry. Since 1997, he has been leading the Center for Ultrafast Optical Characteristics Control through the National Creative Research Initiatives Program supported by the Korea Science Engineering Foundation.

Atsuhiro Osuka (b. 1954) grew up in Gamagori, Aich, Japan. He received a B. S. in chemistry in 1977 and a Ph. D. in 1982 from Kyoto University. After 4 years as an Assistant Professor at Ehime University, he returned to Kyoto University, where he is Professor of Chemistry. Currently he is the leader of the Core Research for Evolutionary Science and Technology Project supported by the Japan Science and Technology Corporation.

10.1021/ar030242e CCC: $27.50
Published on Web 08/12/2004

Chart 1

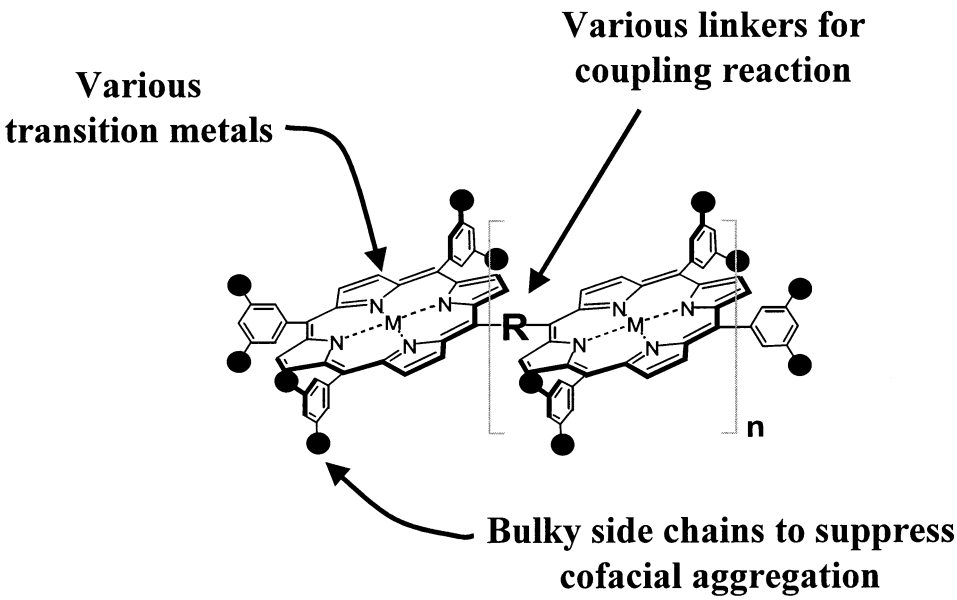

recently been developed by us. Our synthesis of meso−meso-linked diporphyrins by Ag(I)-promoted oxidation of 5,15-diaryl substituted Zn(II) porphyrins opened new synthetic porphyrin chemistry, in which metalloporphyrins with sterically uncongested periphery are converted under appropriate oxidation conditions into a variety of directly linked diporphyrins with varying electronic interactions, depending on the coupling site, attachment modes (singly, doubly, or triply), and central metal. We prepared a wide range of covalently linked diporphyrins and porphyrin arrays, including meso−meso-linked linear porphyrin arrays, two-dimensional windmill arrays, three-dimensional gridlike arrays, strapped meso−meso-linked diporphyrins, and a cyclic array, which are interesting as artificial models in terms of the well-defined arrangement of many porphyrins. Excitonic interactions and photoexcited-state dynamics of these porphyrin arrays have thus been examined by ultrafast time-resolved measurements, which reveal that the meso−meso-linked diporphyrin motif is quite useful not only for attaining excitation energy hops over many porphyrins without an energy sink but also amenable for fine tuning by dihedral angle control. We also prepared fused porphyrin arrays (**T*n***, Chart 2) that are attractive in terms of rigid and coplanar structures and exceptionally low HOMO−LUMO gaps.

2. One-Dimensional meso−meso-Linked Linear Porphyrin Arrays

2.1. Synthesis. Treatment of a Zn(II) 5,15-diarylporphyrin with $AgPF_6$ in $CHCl_3$ gave rise to the formation of meso−meso-linked porphyrin arrays.[5] Taking advantage of high regioselectivity and high solubility, we prepared a series of discrete meso−meso-linked arrays up to 128-mer (**Z*n***, Chart 2) on the basis of iterative dimerization strategy.[6] The Ag(I)-promoted coupling reaction has wide applicability, enabling the synthesis of a wide range of porphyrin arrays including windmill arrays,[7] gridlike arrays,[8] and strapped diporphyrins.[9]

2.2. Exciton Coupling. Despite the direct covalent linkage, the electronic interactions between the neighboring porphyrins are only modest due to the orthogonal conformation of meso−meso-linked porphyrin arrays that disrupt π-electron conjugation. This feature leads to their prospect as artificial light-harvesting antenna and molecular photonic wire in terms of maintenance of individual monomeric porphyrin property.

Figure 1a shows the absorption spectra of **Z*n*** in $CHCl_3$ normalized at the high-energy Soret band around 23 700 to 24 000 cm^{-1}. The Soret bands exhibit splitting due to exciton coupling between the adjacent porphyrin units, while the Q bands remain nearly at the same positions. With an increase in the number of porphyrin moieties, the B_y bands remain nearly at the same positions as those of **Z1** with significant broadening, while the B_x and Q_x bands are continuously red shifted. The absorption spectrum of **Z2** has been interpreted in a qualitative manner by considering two transition dipole moments, B_x and B_y, as shown in Chart 3. Orthogonal conformation of meso−meso-linked porphyrin arrays predicts that, of the four exciton couplings of B_x and B_y, the interaction between B_x and B_x gives rise to allowed transitions and the other three interactions are canceled out (Chart 3). The exciton splitting energy of the neighboring porphyrin units ΔE_0 can be calculated by eq 1

$$\Delta E_0 = \frac{\mu^2}{2\pi\epsilon_0 R^3} \quad (1)$$

where μ is the transition dipole moment of Zn(II) porphyrin and R is the center-to-center distance between the neighboring porphyrins (8.35 Å). The splitting energy (ΔE) for longer arrays are given as eq 2

$$\Delta E = \Delta E_0 \cos[\pi/(N+1)] \quad (2)$$

where N represents the number of porphyrin units in the

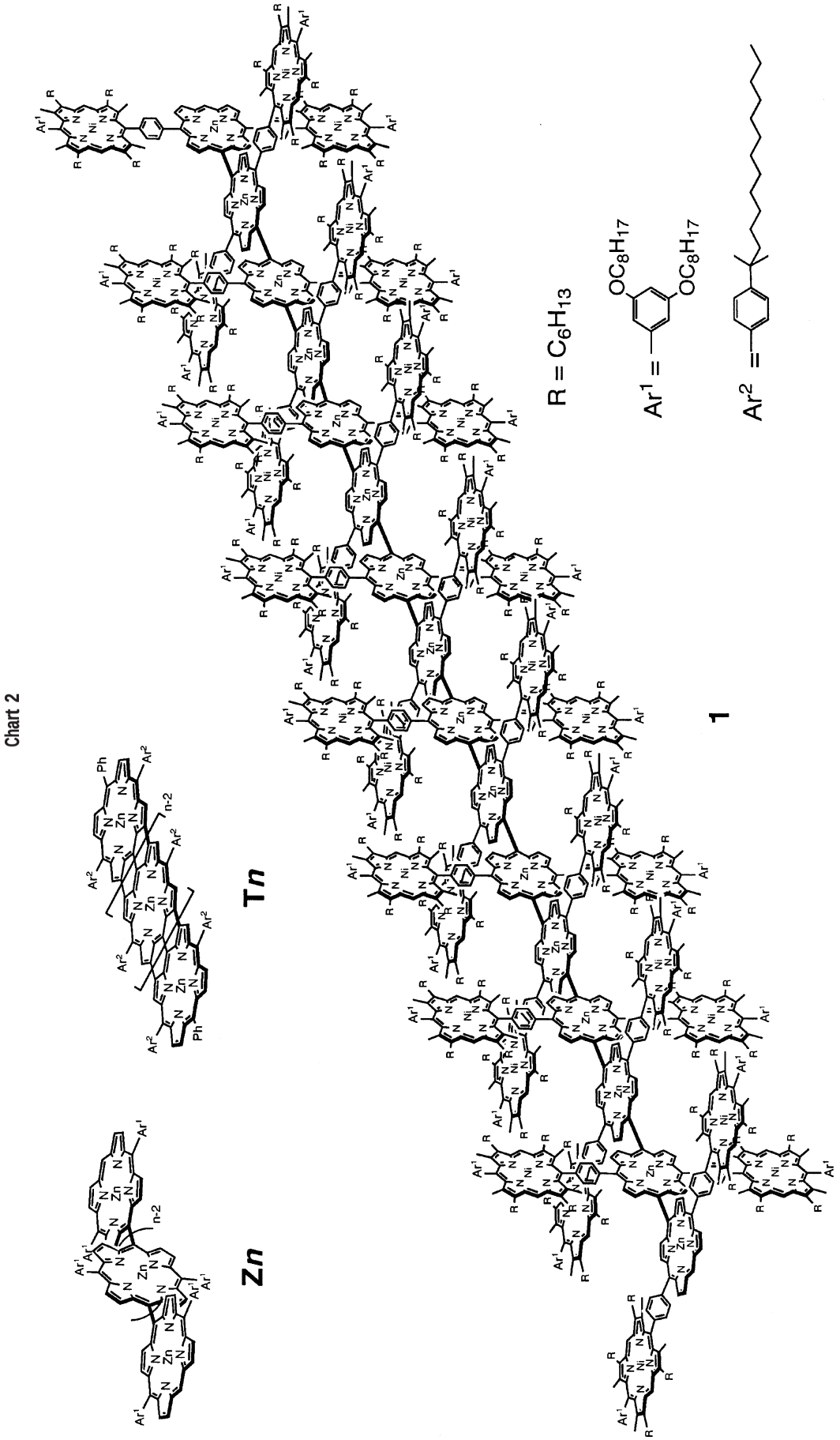
Chart 2
Tn
Zn
1
R = C6H13
Ar1 =
Ar2 =
OC8H17
OC8H17

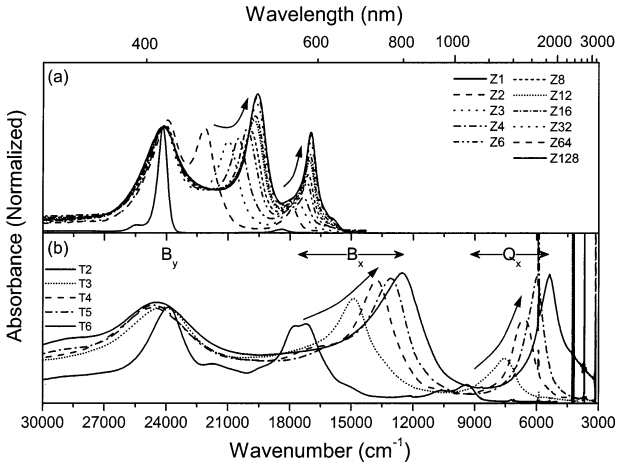

FIGURE 1. UV−vis−IR absorption spectra of (a) the porphyrin monomer and *meso-meso* orthogonally linked Zn(II) porphyrin arrays from **Z2** to **Z128** and (b) fused porphyrin arrays from **T2** to **T6** in $CHCl_3$ at room temperature. The background absorptions at ∼6000, ∼4000, and ∼3500 cm^{-1} in part b result from the overtones of C−H vibration of the solvent.

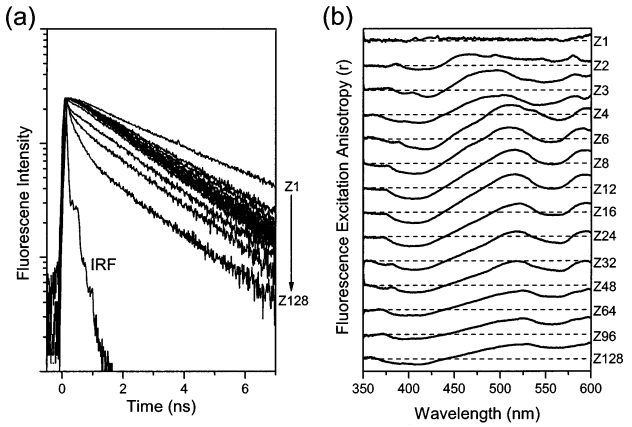

FIGURE 2. The fluorescence decay curves of **Z1**−**Z128** porphyrin arrays in toluene probed by TCSPC technique (a) and the fluorescence excitation anisotropy spectra of corresponding porphyrin arrays **Z1**−**Z128** (b).

array. The observed Soret band splitting energy ΔE exhibits a good linear correlation against $\cos[\pi/(N+1)]$, and the splitting energy ΔE_0 can be determined to be 4 300 cm^{-1} by doubling the observed slope. The observed linear relationship indicates that the constituent porphyrin pigments are aligned in a regular arrangement and that the absorption spectral shapes are actually determined by the number of porphyrin units.[10,11]

In a similar manner, the exciton coupling strength in the S_1 states of the porphyrin arrays was evaluated. The energy differences between the Q(1,0) bands of **Z1** and the porphyrin arrays (**Z2**−**Z16**) were plotted according to eq 1 to obtain a slope of 1140 cm^{-1} (V = 570 cm^{-1}). Interestingly, this value is larger than V = 280 cm^{-1} calculated on an assumption that the through-space dipole−dipole interaction is solely responsible for the electronic coupling. This result thus indicates the presence of through-bond electronic interaction.[11]

2.3. Exciton Coherence Length in Linear Porphyrin Arrays. The coherence length of a strongly coupled

Chart 3

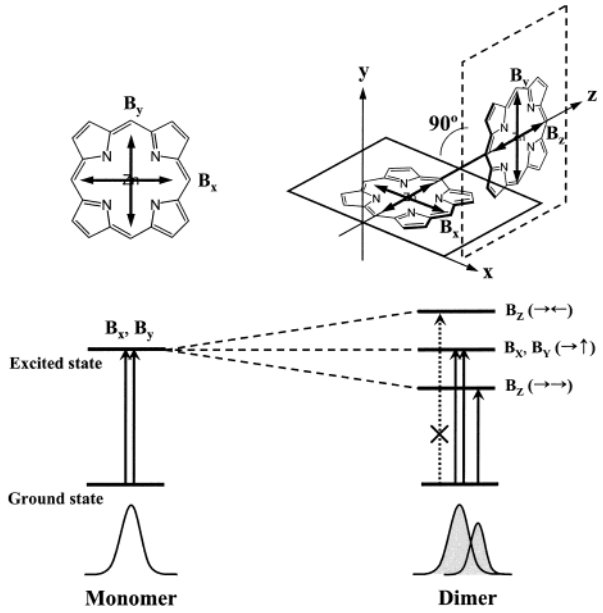

chromophoric aggregate is important in understanding the photoexcited-state dynamics and collective behavior of the transition dipole moments. When the pigments interact with each other and radiate in phase, the radiative decay rate becomes enhanced linearly with the number of pigments. According to the empirical formula for a one-dimensional linear array system,[11] the exciton coherence length (N_c) is estimated by eq 3

$$N_c = 1.38 + 1.33\frac{V}{\gamma} \qquad (3)$$

where V is the electronic coupling and γ is the homogeneous broadening. With the spectral bandwidth of the Q band of Zn(II) TPP at 103 K, γ was estimated to be 250 cm^{-1}. With the estimated V and γ values, we calculated the exciton coherence length (N_c) of porphyrin arrays to be 4.5. Even when the inhomogeneous effects are incorporated (100−150 cm^{-1}), the average exciton coherence length would be 4. Another spectroscopic observable directly related to the exciton coherence length is the radiative coherence length that is defined as the ratio of the radiative decay rates of the array to that of monomer **Z1**. To estimate the radiative coherence length in **Z*n***, the natural radiative decay rates are plotted as a function of the number of porphyrin units. Because the natural radiative decay rate is expected to be proportional to the coherence length and the radiative decay rate of monomer ($k_{arrays} = Nk_{monomer}$), the crossing-point value of approximately 4−5 porphyrin units seems to be a reasonable estimation of the radiative coherence length. This radiative coherence length seems to be compatible with the estimated exciton coherence length in the S_1 states.

2.4. Conformational Heterogeneities in Linear Porphyrin Arrays. The plot of the molar extinction coefficients of **Z*n*** as a function of the number of porphyrin units exhibits a linear summation behavior, indicating the higher absorptivity as the array becomes longer.[6,11] In

Chart 4

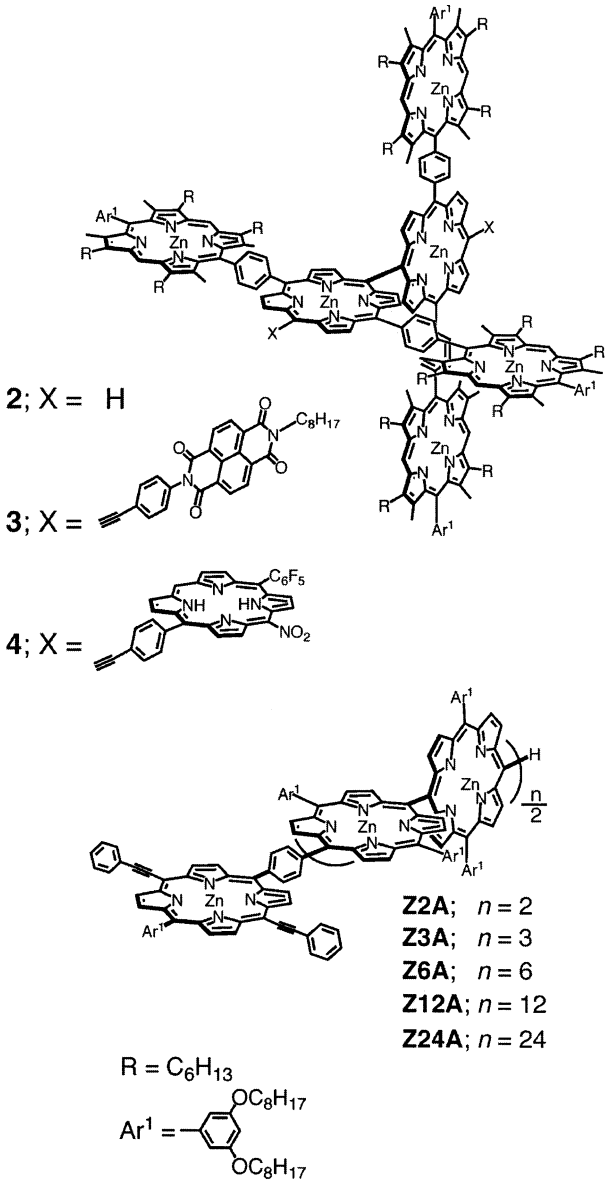

other words, each porphyrin moiety in the array can act as an independent light-absorbing unit. In contrast, the fluorescence quantum yields of **Z*n*** show a maximum value at **Z16** and decrease as the array becomes longer than **Z16**. The fluorescence decay measurements also show a similar trend (Figure 2a). Starting from the fluorescence lifetime of 2.64 ns in **Z1**, the fluorescence lifetimes of **Z*n*** decrease monotonically up to **Z16**.[6,11] In longer porphyrin arrays than **Z16**, the fluorescence temporal profiles start to show double-exponential decay in which the fast-decaying component increases gradually. To reveal this feature, we have recorded the fluorescence excitation anisotropy spectra of **Z*n*** to obtain information on the relative orientation between absorption and emission dipole arrangements in **Z*n*** (Figure 2b). The fluorescence excitation polarization of **Z1** is nearly $^1/_7$ regardless of the excitation wavelength, which is typical when both absorption and emission oscillators are degenerate and polarized in the same plane. In **Z*n***, on the other hand, we observed negative anisotropy values in the fluorescence excitation anisotropy spectra around 413 nm, which corresponds to the high-energy Soret band. The limiting anisotropy value of approximately −0.1 even in longer arrays such as **Z16** indicates a relatively large angle displacement between absorption and emission dipoles upon photoexcitation at ∼413 nm, though this value is still smaller than the orthogonal orientation anisotropy value of −0.2. In longer arrays than **Z16**, this value starts to decrease gradually, but not so significantly (Figure 2b). The anisotropy values above ∼450 nm for **Z*n*** are positive, and the difference between the anisotropy values of ∼413 nm and the entire visible region becomes larger and reaches the maximum at **Z16** and decreases in the arrays longer than **Z16**. The maximum anisotropy value of ∼0.3 above ∼450 nm in **Z16**, which is still slightly smaller than 0.4, for the perfect in-plane orientation between absorption and emission dipoles, indicates a nearly parallel alignment of the absorption and emission dipoles upon photoexcitation at the low-energy exciton split Soret and Q bands. These features indicate that the overall geometries of **Z*n*** remain as linear for <**Z16** and start to deviate from linearity for >**Z16**. AM1 calculation shows that the dihedral angle distribution is estimated to be 90 ± 15° in **Z2** at the ambient temperature. Thus, the summation of the dihedral angle distribution as well as the slight tilting between the adjacent porphyrin rings in longer **Z*n*** gives rise to crooked geometry in longer **Z*n***. Indeed, the scanning tunneling microscopy (STM) measurement of **Z48** shows a curved geometry although the STM image gives more curved structure intrinsically due to multiple interactions of **Z48** with the gold surface. On the basis of our spectroscopic measurements, we conclude that the overall geometries of **Z*n*** start to bend severely for >**Z16**. The systematic decrease in the fluorescence lifetimes of **Z*n*** as the array becomes longer is also consistent with the geometry changes in **Z*n***, because the bent structures in **Z*n*** act as nonradiative quenching sites in excitation energy migration processes.

2.5. EET with meso−meso-Linked Porphyrin Array as an Energy Acceptor. Windmill porphyrin arrays were prepared by the Ag(I)-promoted coupling reaction of 1,4-phenylene-bridged linear porphyrin arrays comprising of a central Zn(II)-β-free porphyrin and flanking peripheral Ni(II)-β-octaalkylporphyrins.[7,8] The coupling reaction was again advantageous in light of its high regioselectivity and easy extension to large porphyrin arrays. The windmill porphyrin arrays in turn served as an effective substrate for further coupling reaction, giving three-dimensionally arranged grid porphyrin arrays, for instance, gridlike porphyrin array **1** (Chart 2). Well-defined three-dimensional arrangements of these porphyrin arrays are interesting from the viewpoint of molecular-based information storage system, where information is stored in the distinct oxidation states.

In Zn(II)-metalated windmill porphyrin array **2** (Chart 4), the energy level of the S_1 state of the meso−meso-linked diporphyrin core is lower than that of the peripheral porphyrins by 0.06 eV, thereby allowing EET from the peripheral porphyrins to the central diporphyrin core with

a EET rate of (30−50 ps)$^{-1}$, which has been confirmed by fluorescence lifetimes in the time-resolved fluorescence measurements.[7,8] The windmill model system has been extended to EET charge separation coupled models **3** and **4** (Chart 4) by attaching 1,4,5,8-naphthalene-tetracarboxydiimide and meso-nitrated free-base porphyrin as electron acceptors to the meso position of the meso−meso-linked diporphyrin core. In these models, a series of photochemical events including EET, charge separation, and hole transfer were realized in a single molecule to provide long-lived charge separated states.[12]

2.6. EET with meso−meso-Linked Porphyrin Array as an Energy Donor. We have investigated the EET processes in **Z*n*A** (***n*** = 1, 2, 3, 6, 12, and 24, Chart 4), in which a *meso*−*meso*′-bisphenylethynylated porphyrin energy acceptor (**A**) is linked to the end meso carbon of **Z*n***.[13] The absorption spectra of hybrid porphyrin arrays in the Q-band region are essentially given by the sum of the absorption spectra of **Z*n*** and **A**, indicating that the electronic interactions in the ground state are relatively weak. This feature enables a selective photoexcitation of the donor to monitor the EET. In addition, the donor emission and the acceptor absorption are well overlapped with each other, which is quite favorable for the rapid energy transfer. The steady-state fluorescence comes only from the acceptor moiety, in **Z1A**−**Z12A**, indicating nearly the quantitative EET. In **Z24A**, which has a molecular length of ca. 217 Å, the fluorescence comes largely from the acceptor moiety and partly from the donor moiety, indicating that the intramolecular EET is not quantitative. The transient absorption spectra of **Z1A**−**Z24A** were taken by selective photoexcitation of **Z*n***, which provided the EET rates from the photoexcited **Z*n*** to acceptor **A**: (2.5 ps)$^{-1}$ for **Z1A**, (3.3 ps)$^{-1}$ for **Z2A**, (5.5 ps)$^{-1}$ for **Z3A**, (21 ps)$^{-1}$ for **Z6A**, (63 ps)$^{-1}$ for **Z12A**, and (108 ps)$^{-1}$ for **Z24A**.[13]

To explain the observed EET rates in **ZnA**, three theoretical models (dipole−dipole (Förster), energy-hopping, and simple quantum-mechanical mechanisms) are considered. First, the EET between donor and acceptor is approximately explained by the point dipole−dipole interactions, the so-called Förster mechanism, assuming that the donor array is considered as a single chromophore. The Förster energy-transfer rates are estimated to be (5.2 ps)$^{-1}$ for **Z1A**, (6.9 ps)$^{-1}$ for **Z2A**, (20 ps)$^{-1}$ for **Z3A**, (160 ps)$^{-1}$ for **Z6A**, (2300 ps)$^{-1}$ for **Z12A**, and (49000 ps)$^{-1}$ for **Z24A**. The estimated EET rates deviate significantly from the observed ones, indicating the assumption that the meso−meso-linked porphyrin array that acts as one chromophore is not appropriate. Second, we consider the energy-hopping model, in which each porphyrin moiety acts as one chromophore, and the EET scheme is given as

$$\mathbf{Z}n\mathbf{-\cdots-Z2^*-Z1-A} \underset{k_{-1}}{\overset{k_1}{\longleftrightarrow}} \mathbf{Zn-\cdots-Z2-Z1^*-A} \xrightarrow{k_2} \mathbf{Z}n\mathbf{-\cdots-Z2-Z1-A^*}$$

This mechanistic model yields pseudo-first-order production because k_1 would be much faster than k_2, which is predictable from the fact that the excitation energy-hopping rate in **Z*n*** is estimated to be (∼0.2 ps)$^{-1}$,[14] and the energy-transfer rate from photoexcited Zn(II)porphyrin to free-base porphyrin in the *meso*−*meso*-phenylene linked porphyrin heterodimer was evaluated to be (∼3 ps)$^{-1}$.[15] On the basis of the above assumptions, we can make following equation

$$\frac{\mathrm{d}\mathbf{A}^*}{\mathrm{d}t} = k_2\mathbf{Z1^*} \approx \frac{k_2}{n} \tag{4}$$

where **A*** and **Z1*** represent the local excited states of **A** and **Z1**, respectively. These are not so outrageous, though they still show some deviations from the observed EET rates.

Third, the energy-transfer rate from simple quantum mechanical treatments can be considered. In our array, the energy-transfer rate (k_N) is expressed by the time-dependent perturbation theory

$$k_N \approx \frac{2}{N+1}\left[\sum_{n=1}^{N}\left(\frac{R_1}{R_n}\right)^3 \sin\left(\frac{\pi}{N+1}n\right)\right]^2 k_1 \tag{5}$$

where N is the number of porphyrin units in the donor array and R_n represents the distance between nth donor and acceptor. Equation 5 was obtained on the assumption that the lowest exciton state is coherently coupled with all molecules in the donor aggregates. This assumption is acceptable when the total number of molecules N is small. When N is large, however, the lowest exciton state should be coherently coupled with only a limited number L, because coherence is easily disrupted over long distance. In this case, the lowest exciton state exists by a number of $N - L + 1$ on the linear array composed of N molecules. Assuming, for simplicity, that the lowest exciton state is realized with the same probability of $1/(N - L + 1)$, eq 5 should be replaced by

$$k_N = k_L/(N - L + 1)$$

when

$$N > L \tag{6}$$

The EET rate relative to that of **Z1A** ($N = 1$) is given by k_1/k_N. When L was set as variable, the most reliable rate constant was calculated for $L = 4$, and the EET rate constants thus calculated are (2.5 ps)$^{-1}$ for **Z1A**, (3.4 ps)$^{-1}$ for **Z2A**, (4.7 ps)$^{-1}$ for **Z3A**, (23 ps)$^{-1}$ for **Z6A**, (70 ps)$^{-1}$ for **Z12A**, and (163 ps)$^{-1}$ for **Z24**. Because the calculated results are in a good agreement with the observed ones, this approach seems to be most suitable, again supporting a view that the excited states of the tightly bound porphyrin arrays should be excitons covering a number of molecules coherently.

As shown above, the EET in **Z24A** is not quantitative. This feature may be partly related to insufficient electronic coupling between the neighboring porphyrins for far-positioned porphyrin chromophores to participate in the EET and to increased tendency to take curved chain geometry in longer **Z*n***. Because such a bent structure gives rise to nonradiative quenching sites that suppress the EET

over the long distance, even longer coherent length than $L = 4$ is expected to work for more rigid geometry of porphyrin array.

2.7. Tuning Electronic Interaction by Dihedral Angle Control. As discussed above, the electronic interaction in meso−meso-linked porphyrin arrays is substantial but only modest, considering the direct covalent linkage. This situation has led to tuning of electronic interactions by dihedral angle control, for which we explored covalent and noncovalent approaches.

In covalent approach, we prepared a series of meso−meso-linked diporphyrins **S*n*** strapped with a dioxymethylene group of various length (n = 10, 8, 6, 5, 4, 3, 2, and 1) by the intramolecular Ag(I)-promoted coupling (Chart 5).[9] The absorption spectrum of relatively unconstrained diporphyrins **S10** strapped with a long-strap chain is similar to that of **Z2**. This has been interpreted in terms of the orthogonal conformation for both diporphyrins (**S10** and **Z2**). Shortening of the strap length causes systematic changes in the absorption spectra, where the intensities of the split Soret bands are decreased and the absorption bands at ca. 400 nm and >460 nm are intensified and a prominent one-band feature of the Q band is changed to a distinct two-bands feature with concurrent progressive red shift of the lowest Q(0,0) band, seemingly reflecting a symmetry change from D_{2d} to D_2. The fluorescence spectra also exhibit systematic changes, roughly tracing the changes of the absorption spectra. The resonance Raman (RR) spectra taken for excitation at 457.9 nm are variable among **S*n***, while the RR spectra taken for excitation at 488.0 nm are rather constant throughout the series.[16−18]

A noncovalent approach utilized the coordination of α,ω-diaminoalkane to zinc(II) centers in the porphyrin core. Among the α,ω-diaminoalkanes examined, 1,7-diaminoheptane was most effective by a 1:1 complexation to distort meso−meso-linked diporphyrin from its orthogonal conformation, which was followed by the absorption and fluorescence changes in a reversible manner. Actually the absorption spectrum of **Z2**:1.7-diaminoheptane complex is similar to that of **S4** with a dihedral angle of 60−70°. When this noncovalent control of the dihedral angle of meso−meso-linked diporphyrin was applied to triporphyrin model **5**, reversible switching of intramolecular EET was achieved (Chart 5).[19] In a free form of **5**, the intramolecular EET proceeds from the meso−meso-linked Zn(II) diporphyrin to the free-base porphyrin with a rate of $(5\ \text{ps})^{-1}$, while the EET was made switched from the free-base porphyrin part to the Zn(II) diporphyrin part with a rate of $(\text{ca. } 10\ \text{ps})^{-1}$ upon complexation with 1,7-diaminoheptane. Further addition of acetic acid restored the original EET from the Zn(II) diporphyrin to the free-base porphyrin, through liberation of 1,7-diaminoheptane from the Zn(II) diporphyrin moiety.

3. EET Phenomena in Two-Dimensional Cyclic Zn(II) Porphyrin Arrays

Inspired by the wheel-like architecture of photosynthetic pigments (LH2 and LH1), particular attention has been focused on the construction of covalently linked cyclic porphyrin arrays, which aid the understanding of the fundamental mechanisms of the EET process in the natural photosynthetic antenna or find new applications as optoelectronic material. The synthetic arrays so far prepared contain at most 6 porphyrins,[20] whereas B800 and B850 in LH2 consist of 9 bacteriochlorophyll *a* (Bchl *a*) and 9 dimeric subunits of Bchl *a*, respectively, and B870 in LH1 is believed to consist of 16 pairs of dimeric Bchl *a*, hence posing a further synthetic challenge.

Recently, we synthesized cyclic porphyrin 12-mer **6** by intramolecular cyclization of linear porphyrin 12-mer under highly dilute condition (Chart 5).[21] The structure of **6** has been confirmed by a variety of spectroscopic methods including the STM detection of a single molecule on the Cu(100) metal surface, which indicated a ring structure with a diameter of ca. 35−36 Å. The absorption spectrum of **6** displays absorption bands at 410−420 and 465 nm through the strong exciton coupling, being similar to those of meso−meso-linked diporphyrins. **6** emits the fluorescence with nearly the same quantum yield as those of linear arrays, indicating no serious quenching in the singlet excited state.

The excited-state dynamics of **6** have been examined in comparison with those of **Z2** using the time-correlated single photon counting (TCSPC), fluorescence anisotropy decay and femtosecond transient absorption anisotropy (TAA) measurements. The fluorescence lifetimes measured by single photon counting are 1.05 ns (30−35%) and 1.81 ns (65−70%) for **6**. The average fluorescence lifetime is then calculated to be 1.56 ns. The fluorescence anisotropy decay measurement revealed the decay components: 72 ps (17%) and 5.4 ns (83%) for **6** and 500 ps (100%) for **Z2**, while the femtosecond time-resolved TAA measurements taken by excitation at 570 nm (Q-band excitation) revealed the decay components: 240 fs (65%) and 1.22 ps (35%) decays for **6** and only a 180-fs component for **Z2**. With more accurate time resolution for the TAA measurement, the shortest anisotropy decays of ca. 180−240 fs for **6** and **Z2** have been assigned to incoherent exciton hopping within meso−meso-linked diporphyrin. On the other hand, the longest decay time of 5.4 ns has been assigned to the rotational diffusion time for **6** because it is much slower than that of **Z2** (500 ps) due to much increased molecular volume of **6**. Finally, the 1.22-ps decaying component for **6** has been assigned to the energy migration time between the **Z2** subunits bridged by a 1,3-phenylene spacer. Because each **Z2** unit in **6** is connected with two adjacent **Z2** units with an angle of $\alpha = 60°$ in a cyclic form, the excitation energy hopping rate constant can be evaluated from $\tau_{\text{depolarization}} = \tau_{\text{hopping}}/4(1 - \cos \alpha^2)$ based on the model employed for LH1 and LH2,[20] resulting in the exciton hopping time of 1.22 ps × 3 = 3.7 ps. The exciton−exciton annihilation processes which are sensitive to excitation photon density can also be directly correlated with the exciton hopping time. Thus the fast component sensitive to pump intensity in transient absorption decay profiles reflects the migration-limited exciton-hopping time. For cyclic porphyrin arrays, the

Chart 5

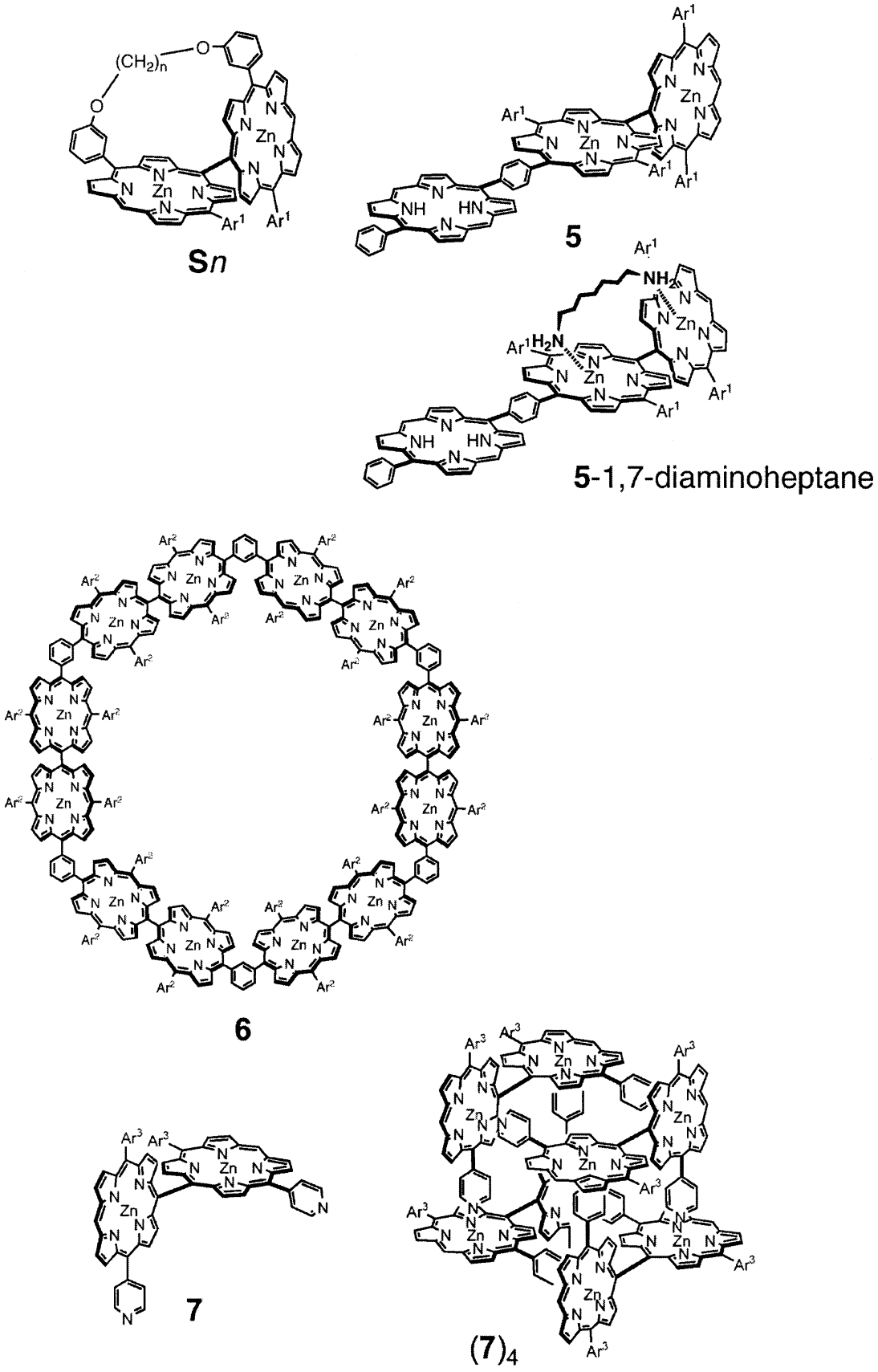

relationship between exciton annihilation and hopping times is given by $\tau_{\text{annihilation}} = [(N^2 - 1)/24]\tau_{\text{hopping}}$, where N represents the number of hopping sites in the cyclic arrays. In our cyclic porphyrin array **6**, the number of

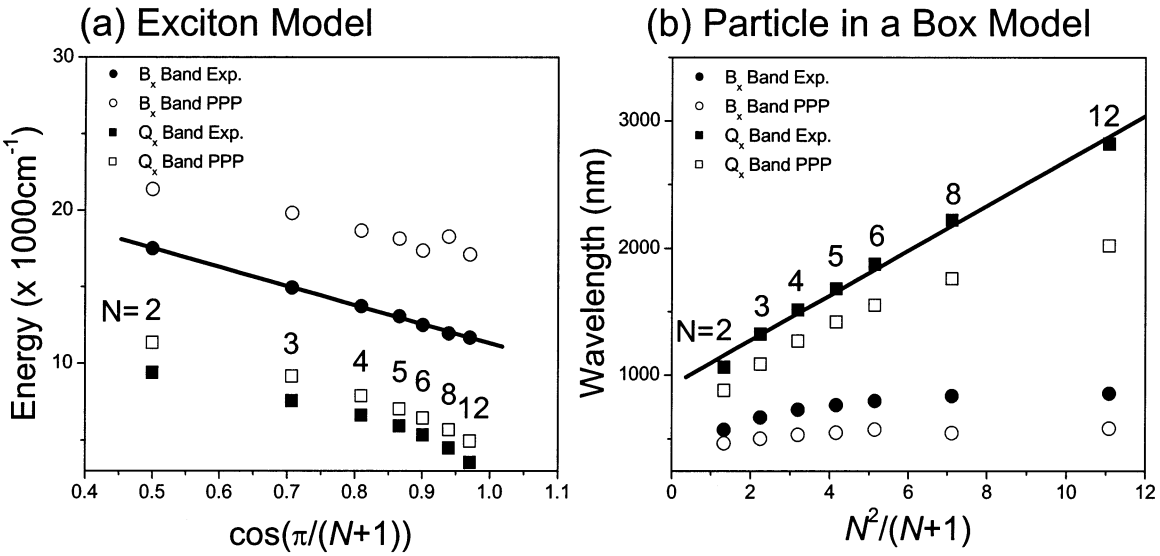

FIGURE 3. Plots of the energies of the absorption bands B_x and Q_x of **T*n*** as a function of the number of porphyrin units show a good correlation between the experimental data and PPP−SCI calculated values. The electronic character of the B_x band is explained by the splitting energy of the exciton model (a) whereas that of the Q_x band is well fitted by a particle in a box model (b).

hopping sites is regarded as six because the directly linked porphyrin dimer unit in **6** is likely to act as a single hopping site due to a strong excitonic coupling between porphyrin monomers arising from a very short center-to-center distance of 8.4 Å. The obtained $\tau_{hopping} = 0.686 \times 6.5$ ps $= 4.5$ ps is similar to the exciton hopping time of 3.7 ps from the transient absorption anisotropy decay, leading to the average exciton hopping time of 4.1 ps for porphyrin cyclic array **6**.

4. EET Phenomena in Three-Dimensional Zn(II) Porphyrin Boxes

A three-dimensional Zn(II) porphyrin box is formed by a self-assembly of **7** that have two pyridyl groups at two meso positions (Chart 5).[22] Owing to the different *meso*-aryl substituents, **7** is chiral. The spontaneous box formation is achieved through self-sorting association of the same enantiomer ((*R*)-**7** + (*R*)-**7** and (*S*)-**7** + (*S*)-**7**) via intermolecular coordination of the Zn(II) central metal ion toward the peripheral pyridyl groups (Chart 5). Because the intermolecular coordination between **7** competes with the solvent coordination as an axial ligand of the Zn(II) porphyrin monomer moiety in **7**, the box formation significantly depends on the solvent polarity. The formation of the box $(\mathbf{7})_4$ occurs in CH_2Cl_2, which has a rigorously rigid structure with a sizable cavity of approximately $10 \times 10 \times 8$ Å^3. Consequently, a much slower rotational diffusion time of ~4.7 ns for the box $(\mathbf{7})_4$ was obtained from the fluorescence anisotropy decay measurements in slow time domain through the TCSPC technique because of its large molecular volume, while **7** in pyridine reveals a rotational diffusion time of ~1.0 ns.

In the box, complicated intra- and intermolecular interactions arise from the dipole−dipole excitonic interactions between eight mutually perpendicular porphyrin molecules. To examine the EET process occurring on a fast time domain, femtosecond TAA decay measurements were performed.[23] While monomeric **7** reveals only slow transient absorption decay without any anisotropy decay in the time region of tens of picosecond, the box $(\mathbf{7})_4$ shows a relatively fast TAA rise of 12 ps. This fast anisotropy rise time is also correlated with the EET time of 12 ps $\times$ 4 = 48 ps from $\tau_{depolarization} = \tau_{hopping}/4(1 - \cos \alpha^2)$ where $\alpha = 90°$ in the box $(\mathbf{7})_4$, indicating the fast EET process that arises from the large excitonic dipole−dipole interactions in the box $(\mathbf{7})_4$. By the same analogy as in the porphyrin cyclic array **6**, the observed slowest exciton−exciton annihilation time of 30 ps gives rise to the hopping time of 30 ps $\times$ 1.6 = 48 ps as the number of hopping sites N in $\tau_{annihilation} = [(N^2 - 1)/24]\tau_{hopping}$ for the box $(\mathbf{7})_4$ is regarded as four. The number of hopping sites of four seems to be reasonable because the directly linked porphyrin dimer unit is likely to act as a single hopping site in the box $(\mathbf{7})_4$. The obtained exciton hopping times from the two separate measurements are consistent with each other.

5. Porphyrin Tapes

A series of meso-meso, $\beta-\beta$, and $\beta-\beta$ triply linked porphyrin arrays (**T*n***, Chart 2) were prepared by the oxidation of the corresponding *meso*−*meso*′-diphenyl capped meso−meso-linked Zn(II) porphyrin arrays with 2,3-dichloro-5,6-dicyano-1,4-benzoquinone (DDQ) and $Sc(OTf)_3$.[24] These fully conjugated porphyrin tapes **T*n*** have planar tape-shaped structures and display drastically red-shifted absorption spectra that reach into the far-IR region (Figure 1b), reflecting the extensive π conjugation. The lowest energy electronic absorption bands become increasingly red shifted and intensified upon the increase of the number of porphyrins and eventually reach the infrared region (Figure 3). Typically, the longest fused array, 12-mer, exhibits a lower-lying electronic transition

band with a peak around 3 500 cm^{-1} tailing to ca. 1 500 cm^{-1}. The one-electron oxidation potentials become also decreased progressively upon the increase of the number of porphyrins (E_{ox}[*V*] vs $AgClO_4/Ag = 0.21$ for 2-mer, −0.09 for 4-mer, and −0.24 for 8-mer). The extremely small HOMO−LUMO gaps, the exceedingly low oxidation potentials, and the linearly long rigid molecular shapes of longer triply linked fused porphyrin arrays encourage their potential usage as a molecular electric wire.

The lowest excited states of the porphyrin tapes decay rapidly to the ground state with the time constants of 4.5 ps for **T2**, 2.3 ps for **T3**, 0.4 ps for **T4**, and 0.3 ps for **T5** and **T6**.[25] These very short lifetimes that can be explained by the energy gap law are interesting with regard to their potential use in all optical switching via the intensity-dependent refractive index changes for optical communications and data-processing applications.[26] They are also promising as novel nonlinear optical materials in view of extensive π conjugation over the entire molecule.

6. Conclusions

The time-resolved spectroscopic measurements are conducted to characterize the rates and yields of excitation energy migration processes in various forms of porphyrin arrays. These results demonstrate that the competition in EET processes can be modulated by the choice of metalloporphyrin and also, by inference, its location in the array. This provides an avenue for achieving different properties and functions of photonic materials based on these arrays. The fundamental information about the excited state dynamics and decay pathways in the porphyrin arrays is essential for properly interpreting the results on more complex arrays, such as two- and three-dimensional porphyrin arrays. The novel porphyrin arrays envisaged will make use of tuned photophysical properties to elicit specific molecular electronic properties.

This work has been financially supported by the National Creative Research Initiatives Program of the Ministry of Science & Technology of Korea. The work at Kyoto was supported by CREST (Core Research for Evolutional Science and Technology) of Japan Science and Technology Corporation (JST). The authors would like to express their sincere gratitude to the talented graduate students, postdoctoral fellows, and collaborators listed as coauthors in the references involved in elaborate synthesis of various porphyrin molecules and very sophisticated measurements of their photophysical properties.

References

(1) McDermott, G. M.; Prince, S. M.; Freer, A. A.; Hawthonthwaite-Lawless, A. M.; Papiz, M. Z.; Cogdell. R. J.; Isaacs, M. W. Crystal Structure of an Integral Membrane Light-Harvesting Complex from Photosynthetic Bacteria. *Nature* **1995**, *374*, 517−521.

(2) Pullerits, T.; Sundström, V. Photosynthetic Light-Harvesting Pigment-Protein Complexes: Toward Understanding How and Why. *Acc. Chem. Res.* **1996**, *29*, 381−389.

(3) Holten, D.; Bocian, D. F.; Lindsey, J. S. Probing Electronic Communication in Covalently Linked Multiporphyrin Arrays. A Guide to the Rational Design of Molecular Photonic Devices. *Acc. Chem. Res.* **2002**, *35*, 57−69 and references are therein.

(4) Kim, D.; Osuka, A. Photophysical Properties of Directly Linked Porphyrin Arrays. *J. Phys. Chem. A.* **2003**, *107*, 8791−8816 and references therein.

(5) Osuka, A.; Shimidzu, H. *meso-meso* Linked Porphyrin Arrays. *Angew. Chem., Int. Ed. Engl.* **1997**, *36*, 135−137.

(6) Aratani, N.; Osuka, A.; Kim, D.; Kim, Y. H.; Jeong, D. H. Extremely Long, Discrete *meso-meso*-Coupled Porphyrin Arrays. *Angew. Chem. Int. Ed.* **2000**, *39*, 1458−1462.

(7) Nakano, A.; Osuka, A.; Yamazaki, I.; Yamazaki, T.; Nishimura, Y. Windmill-Like Porphyin Arrays as Potent Light-Harvesting Antenna Complexes. *Angew. Chem., Int. Ed. Engl.* **1998**, *37*, 3023−3027.

(8) Nakano, A.; Yamazaki, T.; Nishimura, Y.; Yamazaki, I.; Osuka, A. Three-dimensionally Arranged Windmill and Grid Porphyrin Arrays by Ag(I)-Promoted *meso-meso* Block Oligomerization. *Chem.−Eur. J.* **2000**, *6*, 3254−3271.

(9) Yoshida, N.; Jeong, D. H.; Cho, H. S.; Kim, D.; Matsuzaki, Y.; Tanaka, K.; Osuka, A. Fine Tuning of Photophysical Properties of meso-meso Linked Zn(II) Diporphyrins by Dihedral Angle Control. *Chem.−Eur. J.* **2003**, *9*, 58−75.

(10) Cho, H. S.; Song, N. W.; Kim, Y. H.; Jeoung, S. C.; Hahn, S.; Kim, D.; Kim, S. K.; Yoshida, N.; Osuka, A. Ultrafast Energy Relaxation Dynamics of Directly Linked Porphyrin Arrays. *J. Phys. Chem. A* **2000**, *104*, 3287−3298.

(11) Kim, Y. H.; Jeong, D. H.; Kim, D.; Jeoung, S. C.; Cho, H. S.; Kim, S. K.; Aratani, N.; Osuka, A. Photophysical Properties of Long Rodlike *meso-meso* Linked Zinc(II) Porphyrins Investigated by Time-Resolved Laser Spectroscopic Methods. *J. Am. Chem. Soc.* **2001**, *123*, 76−86.

(12) Nakano, A.; Osuka, A.; Yamazaki, T.; Nishimura, Y.; Akimoto, S.; Yamazaki, I.; Itaya, A.; Murakami, M.; Miyasaka, H. Modified Windmill Porphyrin Arrays: Coupled Light-Harvesting and Charge Separation, Conformational Relaxation in the S_1 State, and S_2-S_2 Energy Transfer. *Chem.−Eur. J.* **2001**, *7*, 3134−3151.

(13) Aratani, N.; Cho, H. S.; Ahn, T. K.; Cho, S.; Kim, D.; Sumi, H.; Osuka, A. Efficient Excitation Energy Transfer in Long *meso-meso* Linked Zn(II) Porphyrin Arrays Bearing a 5,15-Bisphenylethynylated Zn(II) Porphyrin Acceptor. *J. Am. Chem. Soc.* **2003**, *125*, 9668−9681.

(14) Min, C.-K.; Joo, T.; Yoon, M.-C.; Kim, C. M.; Hwang, Y. N.; Kim, D.; Aratani, N.; Yoshida, N.; Osuka A. Transient Absorption Anisotropy Study of Ultrafast Energy Transfer in Porphyrin Monomer, its Direct *meso-meso* Coupled Dimer, and Trimer. *J. Chem. Phys.* **2001**, *114*, 6750.

(15) Cho, H. S.; Jeong, D. H.; Yoon, M.-C.; Kim, Y.-R.; Kim, D.; Jeoung, S. C.; Kim, S. K.; Aratani, N.; Shinmori, H.; Osuka, A. Excited-State Energy Transfer Processes in Phenylene- and Biphenylene-Linked and Directly-Linked Zinc(II) and Free-Base Hybrid Diporphyrins. *J. Phys. Chem. A* **2001**, *105*, 4200.

(16) Jeong, D. H.; Yoon, M.-C.; Jang, S. M.; Kim, D.; Cho, D. W.; Yoshida, N.; Aratani, N.; Osuka, A. Resonance Raman Spectroscopic Investigation of Directly Linked Zinc(II) Porphyin Linear Arrays. *J. Phys. Chem. A* **2002**, *106*, 2359−2368.

(17) Jeong, D. H.; Jang, S. M.; Hwang, I.-W.; Kim, D.; Yoshida, N.; Osuka, A. Investigation of Interporphyrin Charge Resonance of Dihedral Angle Controlled Porphyin Dimers by Resonance Raman Spectroscopy and MO Approaches. *J. Phys. Chem. A* **2002**, *106*, 11054−11063.

(18) Cho, H. S.; Song, J. K.; Ha, J.-H.; Cho, S.; Kim, D.; Yoshida, N.; Osuka, A. Comparative Studies on Energy Relaxation Dynamics of Directly Linked Zn^{II} Porphyrin Dimers with Different Dihedral Angles. *J. Phys. Chem. A* **2003**, *107*, 1897−1903.

(19) Shinmori, H.; Ahn, T. K.; Cho, H. S.; Kim, D.; Yoshida, N.; Osuka, A. Dihedral Angle Modulation of *meso-meso* Linked Zn(II) Diporphyrin through Diamine Coordination and Its Application to Reversible Switching of Excitation Energy Transfer. *Angew. Chem.. Int. Ed.* **2003**, *42*, 2754−2758.

(20) Cho, H. S.; Rhee. H.; Song, J. K.; Min, C.-K.; Takasa, M.; Aratani, N.; Cho, S.; Osuka, A.; Joo, T.; D. Kim. Excitation Energy Transport Processes of Porphyrin Monomer, Dimer, Cyclic Trimer, and Hexamer Probed by Ultrafast Fluorescence Anisotropy Decay. *J. Am. Chem. Soc.* **2003**, *125*, 5849−5860.

(21) Peng, X.; Aratani, N.; Takagi, A.; Matsumoto, T.; Kawai, T.; Hwang, I.-W.; Ahn, T. K.; Kim, D.; Osuka, A. A Dodecameric Porphyrin Wheel as a Light-Harvesting Antenna. *J. Am. Chem. Soc.* **2004**, *126*, 4468−4469.

(22) Tsuda, A.; Nakamura, T.; Sakamoto, S.; Yamaguchi, K.; Osuka, A. A Self-Assembled Porphyrin Box from *meso-meso* Linked Bis-{5-p-pyridyl-15-(3,5-di-octyloxyphenyl)porphryinato Zinc(II)}. *Angew. Chem., Int. Ed.* **2002**, *41*, 2817−2821.

(23) Hwang, I.-W.; Cho, H. S.; Jeong, D. H.; Kim, D.; Tsuda, A.; Nakamura, T.; Osuka, A. Photophysical Properties of a Three-Dimensional Zn(II) Porphyin Box. *J. Phys. Chem. B* **2003**, *109*, 9977−9988.

(24) Tsuda, A.; Osuka, A. Fully Conjugated Porphyrin Tapes with Electronic Absorption Bands that Reach into Infrared. *Science* **2001**, *293*, 79−82.
(25) Cho, H. S.; Jeong, D. H.; Cho, S.; Kim, D.; Matsuzaki, Y.; Tanaka, K.; Tsuda, A.; Osuka, A. Photophysical Properties of Porphyrin Tapes. *J. Am. Chem. Soc.* **2002**, *124*, 14642−14654.
(26) Jeong, D. H.; Jang, S. M.; Hwang, I.-W.; Kim, D.; Matsuzaki, Y.; Tanaka, K.; Tsuda, A.; Nakamura, T.; Osuka, A. Resonance Raman Spectroscopic Study of Fused Multiporphyrin Linear Arrays. *J. Chem. Phys.* **2003**, *119*, 5237−5252.

AR030242E